

1 **Rapid sea level rise along the Antarctic margins driven by**
2 **increased glacial discharge**

3
4 **Craig D. Rye*¹, Alberto C. Naveira Garabato¹, Paul R. Holland², Michael P.**
5 **Meredith^{2,3}, A. J. George Nurser⁴, Chris W. Hughes^{5,6}, Andrew C. Coward⁴ and**
6 **David J. Webb⁴**

7
8 **Affiliations**

9 ¹University of Southampton, National Oceanography Centre, Southampton, SO14
10 3ZH, UK.

11 ²British Antarctic Survey, Cambridge, CB3 0ET, UK.

12 ³Scottish Association for Marine Science, Oban, PA37 1QA, UK.

13 ⁴National Oceanography Centre, Southampton, SO14 3ZH, UK.

14 ⁵School of Environmental Sciences, University of Liverpool, Liverpool, UK.

15 ⁶National Oceanography Centre, Liverpool, L3 5DA, UK.

16
17 ***Corresponding author: c.rye@noc.soton.ac.uk**

18
19 **The Antarctic subpolar seas are of great climatic importance due to their**
20 **vigorous interactions with the atmosphere and cryosphere, which influence**
21 **continental deglaciation, global sea level, and the production of dense bottom**
22 **waters. However, understanding these interactions and their impacts is**
23 **confounded by sea ice, which blankets the region seasonally. In particular, the**
24 **regional oceanic response to recent changes in Antarctic freshwater discharge is**
25 **largely unknown. Here, we use satellite measurements of sea surface height**
26 **(SSH) during ice-free months and an ocean circulation model to show that over**
27 **the last two decades (1992-2011) Antarctic coastal sea level has risen at least $2 \pm$**
28 **0.8 mm yr^{-1} above the regional mean south of 50°S , and that this signal is a steric**
29 **adjustment to increased glacial melt from Antarctica. Our findings document the**
30 **strength of the sea level response to accelerating Antarctic discharge, and**
31 **demonstrate a significant climatic perturbation to the cryospheric forcing of the**
32 **Southern Ocean.**

33

34 The Antarctic subpolar seas are a region of intense and complex interactions between
35 the atmosphere, ocean and cryosphere, with an influence on Earth's climate that is
36 greatly disproportionate to their area. Air-sea-ice interactions in these seas are central
37 to the stability of the Antarctic Ice Sheet and global sea level^{1,2}, the volume and extent
38 of Antarctic sea ice³, the Earth's albedo⁴, and the generation of the Antarctic Bottom
39 Water (AABW) that cools and ventilates much of the global ocean abyss⁵. The
40 subpolar seas are currently experiencing a significant increase in freshwater discharge
41 from the grounded Antarctic Ice Sheet¹ and its fringing ice shelves^{1,2,6}. The current
42 state of knowledge concerning the impact on the adjacent ocean of this rapid change
43 in freshwater forcing is, however, extremely limited, consisting of a few suggestive,
44 yet highly localised and temporally sparse time series of *in situ* hydrographic
45 observations⁷⁻¹³. Here, we use multiple lines of evidence (satellite measurements of
46 SSH, *in situ* hydrographic measurements, and results from ocean model simulations)
47 to reveal the local response to the recent Antarctic freshwater imbalance.

48

49 The grounded Antarctic Ice Sheet is currently losing mass overall through increased
50 ice discharge, but gaining mass in places through enhanced snowfall^{1,14}. With modest
51 variability in evaporation and precipitation in subpolar waters¹⁵, the increased
52 discharge is expected to freshen the nearby ocean. Such freshening should be
53 attributable to an 'excess' freshwater discharge above a baseline rate consistent with a
54 steady ocean salinity. Discharge from the grounded ice sheet increased by 150 ± 50
55 Gt yr⁻¹ between 1992 and 2010 (ref. 14), implying an average of 75 ± 25 Gt yr⁻¹
56 excess discharge. An alternative estimate of the grounded ice contribution can be
57 derived by assuming that the excess discharge is equal to net losses from West

58 Antarctica and the Antarctic Peninsula, which sum to $85 \pm 30 \text{ Gt yr}^{-1}$ between 1992
59 and 2011 (ref. 1). Additional mass loss is occurring via the thinning of floating ice
60 shelves. Whilst this mass loss is more uncertain than that of grounded ice, it may be
61 estimated from satellite measurements and modelled surface accumulation, which
62 indicate floating ice thinning of $280 \pm 50 \text{ Gt yr}^{-1}$ between 2003 and 2008 (ref. 16-17)
63 and $115 \pm 43 \text{ Gt yr}^{-1}$ for 1994-2008 (ref. 6). Finally, a series of large ice-shelf retreats
64 has occurred along the Antarctic Peninsula that is not included in the previous figures,
65 and which averages $210 \pm 27 \text{ Gt yr}^{-1}$ between 1988 and 2008 (ref. 6). However, it is
66 unclear how much of the freshwater from these breakups was injected into the ocean
67 over the Antarctic subpolar seas, and how much removed to distance by icebergs. All
68 the above estimates represent changes since the early 1990s, but *in situ* measurements
69 suggest that the ocean was already freshening then, so these values constitute a lower
70 bound for the actual excess discharge above a ‘steady salinity’ rate.

71

72 The excess freshwater flux to the Antarctic subpolar seas in the last two decades is
73 estimated hereafter as the sum of mass losses from the thinning of grounded and
74 floating ice, $\sim 350 \pm 100 \text{ Gt yr}^{-1}$. The bulk of this discharge is focussed around the
75 Antarctic Peninsula and the Amundsen Sea. This excess freshwater input is
76 anticipated to freshen the Antarctic subpolar seas, and to raise regional sea level
77 through both steric (density-induced) and barystatic (mass-induced) effects.
78 Consistent with this, the few available time series of *in situ* hydrographic
79 measurements, collated in Figure 1, suggest that Antarctic subpolar waters have
80 undergone a marked freshening (by $O(0.01)$ per decade) in recent decades⁷⁻¹³. An
81 important limitation of these observations is their strong spatial bias to the Ross Sea,
82 where tracer analyses suggest the implication of glacial meltwater in inducing the

83 local freshening⁷. If the freshening is as widespread as suggested by the very sparse *in*
84 *situ* measurements, and if the increase in Antarctic freshwater discharge is indeed the
85 causal factor, we expect sea level rise to be especially pronounced across the
86 Antarctic subpolar seas, and to occur at a rate commensurate with the increase in
87 freshwater input modulated by ocean dynamics.

88

89 To test this, we examine the evolution of sea level around Antarctica over the last two
90 decades using satellite measurements of SSH. The primary data analyzed are gridded
91 Maps of Sea Level Anomaly (MSLA) generated by AVISO (Archiving, Validation,
92 and Interpretation of Satellite Oceanographic Data) for 1992-2011 (ref. 18; analysis
93 methods and uncertainties are discussed in detail in Suppl. Mat.). Satellite-derived
94 measurements of sea level cannot be readily obtained in the presence of sea ice, so
95 our analysis focuses on the largely ice-free summer months (January-April). Using
96 data from these months, the linear trend in SSH was derived and the global-mean rate
97 of sea level rise for summer months ($\sim 3.2 \text{ mm yr}^{-1}$ between 1992 and 2012)
98 subtracted to reveal the local anomaly (Fig. 1).

99

100 Over the mid-latitude Southern Ocean, the sea level rise anomaly varies zonally, with
101 alternating sign (Fig. 1a). This pattern arises from the superposition of sea level
102 impacts caused by various large-scale modes of atmospheric variability¹⁹. At high
103 latitudes (south of $\sim 62^\circ\text{S}$), however, our analysis reveals a circumpolar,
104 topographically-influenced signal of anomalously rapid sea level rise that has not
105 been observed previously (Fig. 1b), occurring at $1\text{-}5 \text{ mm yr}^{-1}$ above the global mean,
106 with local peaks in the Ross Sea and Prydz Bay. The northern boundary of this rapid
107 sea level rise is identified here as the line where the SSH trend anomaly first changes

108 sign or reaches a minimum with increasing distance from Antarctica (Fig. 1a). The
109 mean sea level rise south of this boundary is at least $2 \pm 0.8 \text{ mm yr}^{-1}$ above the
110 regional mean south of 50°S ($1.2 \pm 1.5 \text{ mm yr}^{-1}$ above the global-mean sea level rise).
111 Whilst the signal covers the broad Antarctic subpolar seas, the signals are most
112 significant over the continental shelves, which are our primary focus.

113

114 Although its statistical significance appears modest, the above quantification is a
115 highly conservative estimate of the regional sea level rise anomaly induced by
116 freshwater forcing. This is because the global-mean rate of sea level rise contains a
117 large thermosteric contribution from the low- and mid-latitude oceans that is unrelated
118 to polar processes²⁰⁻²¹. A more appropriate approach to isolating the local effect of
119 Antarctic freshwater discharge would entail the subtraction of the global-mean rate of
120 barystatic sea level rise from the measured SSH trend (see Suppl. Mat.). This rate is
121 unlikely to exceed 1.5 mm yr^{-1} (ref. 16, 20-21), resulting in a mean sea level rise
122 across the Antarctic subpolar seas of $2.8 \pm 1.5 \text{ mm yr}^{-1}$ above the global barystatic
123 mean. However, the global-mean rate of barystatic sea level rise has substantial
124 uncertainty, so hereafter we consider only the more conservative estimate relative to
125 the global-mean rate of sea level rise.

126

127 The temporal progression and regional distribution of SSH change across the
128 Antarctic subpolar seas (Fig. 2) reveal several important features. For example, SSH
129 displays a pronounced seasonal cycle that is most likely forced by seasonal
130 fluctuations in upper-ocean temperature and salinity²². While this seasonal cycle is
131 larger than the interdecadal sea level rise anomaly, it is distinct from the latter: the
132 linear trend in SSH anomaly affects all stages of the seasonal cycle (see Suppl. Mat.).

133

134 To assess whether the enhanced rate of sea level rise measured across the Antarctic
135 subpolar seas is consistent with forcing by the recent acceleration in glacial discharge
136 from Antarctica, we consider three distinct lines of evidence. First, we use a global
137 ocean circulation model forced with realistic rates of Antarctic freshwater discharge
138 to simulate the regional response to increased discharge (see Suppl. Mat.). All model
139 experiments produce a striking, circumpolar, steric sea level rise anomaly across the
140 Antarctic subpolar seas that strongly resembles the altimetric observations, with a
141 subpolar sea-average anomalous rise of 1-5 mm yr⁻¹ for a freshwater release of ~300
142 Gt yr⁻¹ (the approximate excess Antarctic freshwater discharge averaged over the last
143 20 years) centred in the Amundsen-Bellingshausen sector (Fig. 3). Remarkably, the
144 modelled anomalous SSH signal is comprised of comparable halosteric and
145 thermosteric contributions, with the former being focussed in the upper ocean and the
146 latter at depth. Thus, the model suggests that the directly-forced halosteric sea level
147 rise around Antarctica is amplified by a positive thermosteric feedback. The barystatic
148 contribution of increased Antarctic freshwater discharge to the spatial distribution of
149 the sea level rise signal is shown to be negligible by the simulations.

150

151 Second, we quantitatively compare the altimetric results with recent observational
152 estimates of steric sea level rise around Antarctica. The altimetric rates of Antarctic
153 coastal sea level rise anomaly are found to be in broad agreement with (slightly
154 exceeding) the halosteric sea level rise contribution of ~0.5-3 mm yr⁻¹ implied by the
155 available *in situ* measurements of interdecadal upper-ocean freshening around
156 Antarctica⁷⁻¹³ (Fig. 1 and Suppl. Mat.), in line with model predictions of an important
157 upper-ocean halosteric contribution to the anomalous SSH signal. Similarly, Southern

158 Ocean deep and bottom waters have warmed significantly in the period of our study,
159 inducing a thermosteric sea level rise of $\sim 1 \text{ mm yr}^{-1}$ (ref. 23) that is comparable to the
160 signal discussed here. While the spatial footprint of the deep thermosteric change
161 extends well beyond the Antarctic subpolar seas²³, in poor agreement with our
162 observed signal and model results, the lack of spatial correspondence between
163 thermosteric effects and regional sea level trends may relate to other factors, such as
164 changes in wind forcing or self-gravitation (see Suppl. Mat). Thus, the existence of a
165 significant contribution of deep-ocean thermosteric adjustment to the observed
166 Antarctic coastal sea level rise does not conflict with available observations.

167

168 Third, if it is assumed, based on the preceding modelling and observational evidence,
169 that the Antarctic coastal sea level rise signal is partitioned approximately equally
170 between a directly-forced halosteric component and a positive thermosteric feedback,
171 the excess freshwater input required to explain the measured signal may be estimated.
172 This involves multiplying half the linear trend in ocean volume inside the signal's
173 boundary ($11.6 \text{ km}^3 \text{ yr}^{-1}$; 1.4 mm yr^{-1}) by a modified 'Munk multiplier' (36.7; ref. 24;
174 see Suppl. Mat.), indicating a requirement of $430 \pm 230 \text{ Gt yr}^{-1}$ of excess freshwater
175 input above the nominal rate needed to maintain a steady ocean salinity. This agrees
176 with the increase in Antarctic melt observed in the last two decades ($\sim 350 \pm 100 \text{ Gt}$
177 yr^{-1}), and lends support to our initial hypothesis that the recent imbalance in the
178 Antarctic cryosphere is driving pronounced and widespread changes in the salinity of
179 the high-latitude Southern Ocean.

180

181 Finally, we note that the observed anomalous SSH signal may also be influenced by
182 several tertiary forcing mechanisms, which may account for at most $\sim 10\%$ of the

183 signal and are discussed comprehensively in Suppl. Mat. The most significant of these
184 is the ocean's barystatic response to wind forcing. The gravitational effect of
185 Antarctic ice mass loss reduces relative sea level rise in the Amundsen and
186 Bellingshausen seas by $\sim 1 \text{ mm yr}^{-1}$ (ref. 25). Other mechanisms, such as upper-ocean
187 warming, precipitation-induced freshening or the ocean's barystatic response to the
188 acceleration in Antarctic freshwater discharge, were found to be insignificant.

189

190 In summary, austral summer satellite altimetry measurements show a pronounced
191 circumpolar rise in sea level across the Antarctic subpolar seas that significantly
192 exceeds the global mean. The trend contains a significant halosteric contribution that
193 originates in the increasing discharge of freshwater from Antarctica. Thermosteric sea
194 level rise from the observed warming of the deep Southern Ocean, which has itself
195 been linked to the freshening of the shelf waters ventilating AABW (ref. 23,26; see
196 also Suppl. Mat.), also contributes to the signal. Our findings therefore reveal that the
197 accelerating discharge from the Antarctic ice sheet has had a pronounced and
198 widespread impact on the adjacent subpolar seas over the last two decades, and
199 indicate that a significant climatic perturbation to the cryospheric forcing of the
200 Southern Ocean is underway. Given the key dependence of the Southern Ocean on
201 freshwater forcing, this perturbation has major implications for the region's
202 stratification, circulation and important biogeochemical and ecological processes²⁶⁻²⁹.

203

204

205 **References**

206

207 1 Shepherd, A. *et al.* A reconciled estimate of ice-sheet mass balance. *Science*
208 **338**, 1183-1189,

209

210 2 Shepherd, A., Wingham, D. & Rignot, E. Warm ocean is eroding West
211 Antarctic Ice Sheet. *Geophys. Res. Lett.* **31**, L23402,

212

- 213 3 Parkinson, C. L. & Cavalieri, D. J. Antarctic sea ice variability and trends,
214 1979-2010. *Cryosphere* **6**, 871-880,
215
- 216 4 Meehl, G. A. & Washington, W. M. CO₂ climate sensitivity and snow-sea-ice
217 albedo parameterization in an Atmospheric GCM coupled to a mixed-layer
218 ocean model. *Climatic Change* **16**, 283-306,
219
- 220 5 Orsi, A. H., Johnson, G. C. & Bullister, J. L. Circulation, mixing, and
221 production of Antarctic Bottom Water. *Prog. Oceanogr.* **43**, 55-109,
222
- 223 6 Shepherd, A. *et al.* Recent loss of floating ice and the consequent sea level
224 contribution. *Geophys. Res. Lett.* **37**, L13503
225
- 226 7 Jacobs, S. S., Giulivi, C. F. & Mele, P. A. Freshening of the Ross Sea during
227 the late 20th century. *Science* **297**, 386-389,
228
- 229 8 Jacobs, S. S. & Giulivi, C. F. Large multidecadal salinity trends near the
230 Pacific-Antarctic continental margin. *J. Clim.* **23**, 4508-4524,
231
- 232 9 Aoki, S., Rintoul, S. R., Ushio, S., Watanabe, S. & Bindoff, N. L. Freshening
233 of the Adélie Land Bottom Water near 140°E. *Geophys. Res. Lett.* **32**, L23601
234
- 235 10 Johnson, G. C., Purkey, S. G. & Bullister, J. L. Warming and freshening in the
236 abyssal Southeastern Indian Ocean*. *J. Clim.* **21**, 5351-5363,
237
- 238 11 Ozaki, H., Obata, H., Naganobu, M. & Gamo, T. Long-term bottom water
239 warming in the north Ross Sea. *J. Oceanogr.* **65**, 235-244,
240
- 241 12 Hellmer, H. H., Huhn, O., Gomis, D. & Timmermann, R. On the freshening of
242 the northwestern Weddell Sea continental shelf. *Ocean. Sci.* **7**, 305-316,
243
- 244 13 Williams, G. D., Aoki, S., Jacobs, S. S., Rintoul, S. R., Tamura, T. & Bindoff
245 N. L. Antarctic Bottom Water from the Adélie and George V Land coast, East
246 Antarctica (140–149°E). *J. Geophys. Res.* **115**, C4, C04027
247
- 248 14 Rignot, E., Velicogna, I., van den Broeke, M. R., Monaghan, A. & Lenaerts, J.
249 T. M. Acceleration of the contribution of the Greenland and Antarctic Ice
250 Sheets to sea level rise. *Geophys. Res. Lett.* **38**, L05503,
251
- 252 15 Bromwich, D. H., Nicolas J. P. & Monaghan A. J. An Assessment of
253 Precipitation Changes over Antarctica and the Southern Ocean since 1989 in
254 Contemporary Global Reanalyses. *J. Clim.* **24**, 4189–4209,
255
- 256 16 Depoorter, M. A., Bamber, J. L., Griggs, J. A., Lenaerts, J. T. M., Ligtenberg,
257 S. R. M., van den Broeke, M. R. & Moholdt G. Calving fluxes and basal melt
258 rates of Antarctic ice shelves. *Nature* **502**, 89–92,
259
- 260 17. Rignot E., Jacobs, S., Mouginit, J. & Scheuch B. Ice-shelf melting around
261 Antarctica. *Science* **341** 266-270
262

- 263 18. Le Traon, P. Y., Nadal, F. & Ducet, N. An improved mapping method of
264 multisatellite altimeter data. *J. Atmos. Ocean. Tech.* **15**, 522-534,
265
- 266 19. Spence, P., Fyfe, J. C., Montenegro, A. & Weaver, A. J. Southern Ocean
267 response to strengthening winds in an eddy-permitting global climate model.
268 *J. Clim.* **23**, 5332-5343,
269
- 270 20. Leuliette, E. W. & Miller L. Closing the sea level rise budget with altimetry,
271 Argo, and GRACE. *Geophys. Res. Lett.* **36**, L04608,
272
- 273 21. Gregory, J. M., White, N. J., Church, J. A., Bierkens, M. F. P., Box, J.
274 E., van den Broeke, M. R., Cogley, J. G., Fettweis, X., Hanna, E.,
275 Huybrechts, P., Konikow, L. F., Leclercq, P. W., Marzeion, B., Oerlemans, J.,
276 Tamisiea, M. E., Wada, Y., Wake, L. M. & van de Wal, R. S. W. Twentieth-
277 Century Global-Mean Sea Level Rise: Is the Whole Greater than the Sum of
278 the Parts? *J. Clim.* **26**, 4476–4499.
279
- 280 22. Meredith, M. P., Renfrew, I. A., Clarke, A., King, J. C. & Brandon, M. A.
281 Impact of the 1997/98 ENSO on upper ocean characteristics in Marguerite
282 Bay, western Antarctic Peninsula. *J. Geophys. Res.* **109**, C09013
283
- 284 23 Purkey, S. G. & Johnson, G. C. Antarctic Bottom Water warming and
285 freshening: Contributions to sea level rise, ocean freshwater budgets, and
286 global heat gain. *J. Clim.* **26**, 6105–6122.
287
- 288 24 Munk, W. Ocean freshening, sea level rising. *Science* **300**, 2041-2043,
289
- 290 25 Riva, R. E. M., Bamber, J. L., Lavallée, D. A. & Wouters, B. Sea-level
291 fingerprint of continental water and ice mass change from GRACE. *Geophys.*
292 *Res. Lett.* **37**, L19605,
293
- 294 26 Purkey, S. G. & Johnson, G. C. Global contraction of Antarctic Bottom Water
295 between the 1980s and 2000s. *J. Clim.* **25**, 5830-5844,
296
- 297 27 Dierssen, H. M., Smith, R. C. & Vernet M. Glacial meltwater dynamics in
298 coastal waters west of the Antarctic Peninsula. *Proc. Natl. Acad. Sci.*
299 **19**, 99(4):
300
- 301 28 Boyd, P. W., & Ellwood, M. J. The biogeochemical cycle of iron in the
302 ocean. *Nat. Geosci.*, **3**, 675–682
303
- 304 29 Stammerjohn, S. E., D. G. Martinson, R. C. Smith & R. A. Ianuzzi, Sea ice in
305 the western Antarctic Peninsula region: Spatio-temporal variability from
306 ecological and climate change perspectives. *Deep-Sea Res. II*, **55**, 2041–2058
307 (2008).
308
309
310
311
312

313 **Supplementary information** is linked to the online version of the paper at
314 www.nature.com/nature

315

316 **Acknowledgements** We thank Jeff Blundell for technical help and Adam Blaker for
317 assistance with modelling. We are grateful to Alexander Brearley, Harry Bryden,
318 John Church, Sybren Drijfhout, Pierre Dutrieux, Ivan Haigh, Loïc Jullion, Chris
319 O'Donnell, Maïke Sonnewald and Carl Wunsch for insightful comments and
320 discussions at various stages of this work.

321

322 **Author Contributions** C.D.R. conducted the data analysis, with regular input from
323 A.C.N.G., A.J.G.N., C. W. H., M.P.M. and P.R.H. All these authors contributed to the
324 writing of the manuscript. A.C.C. and D.J.W. assisted with the modelling component
325 of the work.

326 **Author Information** The altimetry data used in the study is available via the AVISO
327 website (<http://www.aviso.oceanobs.com/en/>) as well as the MyOcean website
328 (<http://www.myocean.eu.org/>). The reanalysis wind data is available via the ECMWF
329 website (<http://www.ecmwf.int/>). Reprints and permissions information is available at
330 www.nature.com/reprints. Correspondence and requests for materials should be
331 addressed to c.rye@noc.soton.ac.uk.

332

333

334

335 **Figure legends:**

336

337 **Figure 1 | Regional anomaly in summer (January to April) sea level trend, 1992-**
338 **2011.** The anomaly is calculated relative to the full (barystatic and steric) global-mean
339 rate of sea level rise for summer months. **a.** Circumpolar view, showing the northern
340 boundary of the sea level anomaly in black. Markers indicate *in situ* estimates of
341 interdecadal freshening, shaded by the magnitude of the corresponding halosteric sea
342 level rise. The information for each marker is given in the table in c. The 3000-m
343 isobath is shown in green. **b.** Zonal-mean regional sea level rise. Shading highlights
344 the 2- σ zonal variation.

345

346 **Figure 2 | Time series of sea level anomaly in the Antarctic subpolar seas, 1992-**
347 **2011.** Dotted lines show the full time series, and solid lines the ice-free summer
348 month record. Black: circumpolar average south of the signal's boundary (trend = 1.2
349 mm yr⁻¹); light blue: Bellingshausen and Amundsen seas (BA; 135-60°W; trend = 0.2
350 mm yr⁻¹); dark blue: Ross Sea (RS; 130°E-135°W; trend = 1.3 mm yr⁻¹); red:
351 Australian-Antarctic basin (AA; 50-130°E; trend = 1.9 mm yr⁻¹); green: Amery Basin
352 (AB; 10-50°E; trend = 1.0 mm yr⁻¹); pink: Weddell Sea (WS; 60°W-10°E; trend = 0.5
353 mm yr⁻¹).

354

355 **Figure 3 | Ocean model simulation of the regional anomaly in sea level trend,**
356 **1992-2007.** This is generated by subtracting a control run with a 'background'
357 Antarctic freshwater forcing from an experimental run perturbed by an excess
358 Antarctic freshwater runoff of 300 Gt yr⁻¹ (see Suppl. Mat.). The 3000-m isobath is
359 indicated in green.

360

361
 362
 363
 364
 365
 366
 367
 368
 369
 370
 371
 372
 373
 374
 375
 376
 377
 378
 379
 380
 381
 382
 383
 384
 385
 386
 387
 388
 389
 390
 391
 392
 393
 394
 395
 396
 397
 398
 399
 400
 401
 402
 403
 404
 405
 406
 407
 408
 409
 410
 411

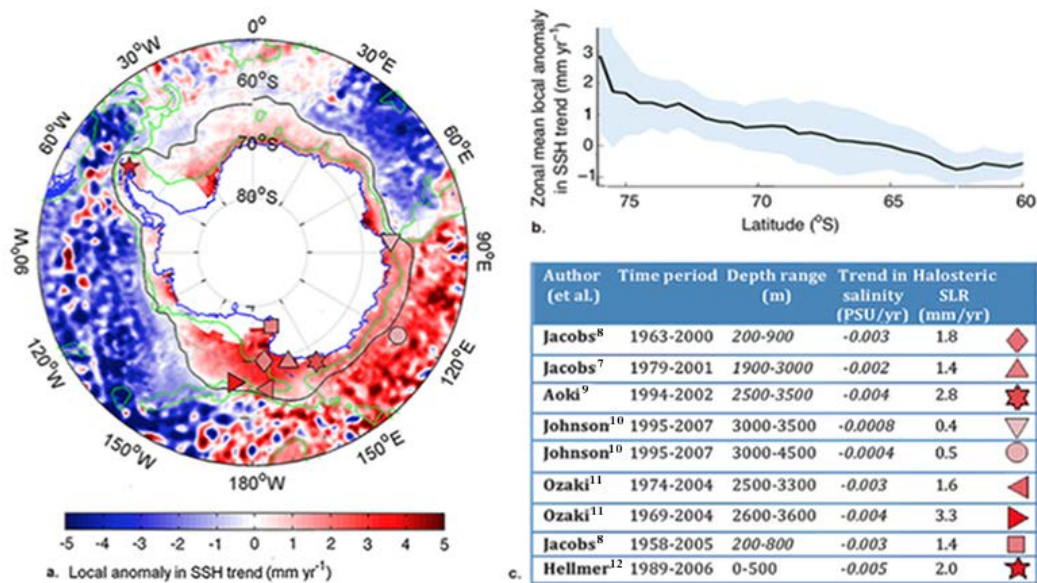
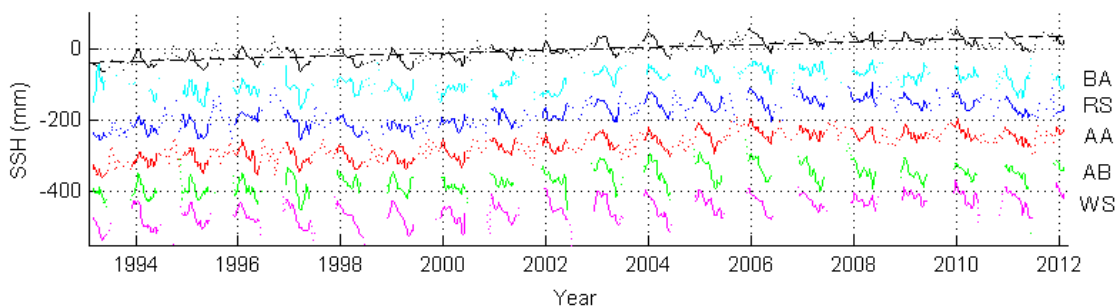


Figure 1 | Regional anomaly in summer (January to April) sea level trend, 1992-2011. The anomaly is calculated relative to the full (barystatic and steric) global-mean rate of sea level rise for summer months. **a.** Circumpolar view, showing the northern boundary of the sea level anomaly in black. Markers indicate *in situ* estimates of interdecadal freshening, shaded by the magnitude of the corresponding halosteric sea level rise. The information for each marker is given in the table in c. The 3000-m isobath is shown in green. **b.** Zonal-mean regional sea level rise. Shading highlights the 2- σ zonal variation.



412
413
414
415
416
417
418
419
420
421
422
423
424
425
426
427
428
429
430
431
432
433
434
435
436
437
438
439
440
441
442
443
444
445
446
447
448
449
450
451
452
453

Figure 2 | Time series of sea level anomaly in the Antarctic subpolar seas, 1992-2011. Dotted lines show the full time series, and solid lines the ice-free summer month record. Black: circumpolar average south of the signal's boundary (trend = 1.2 mm yr⁻¹); light blue: Bellingshausen and Amundsen seas (BA; 135-60°W; trend = 0.2 mm yr⁻¹); dark blue: Ross Sea (RS; 130°E-135°W; trend = 1.3 mm yr⁻¹); red: Australian-Antarctic basin (AA; 50-130°E; trend = 1.9 mm yr⁻¹); green: Amery Basin (AB; 10-50°E; trend = 1.0 mm yr⁻¹); pink: Weddell Sea (WS; 60°W-10°E; trend = 0.5 mm yr⁻¹).

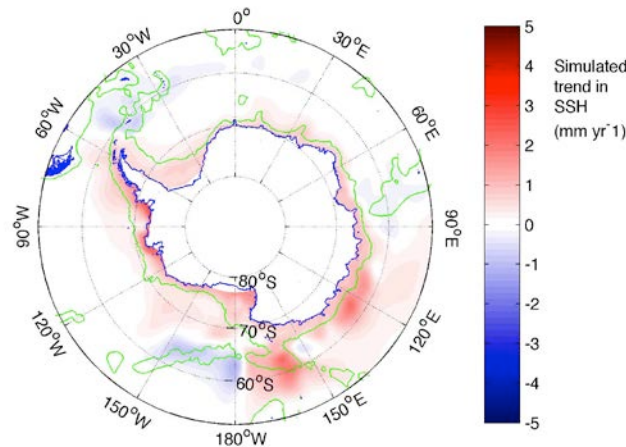


Figure 3 | Ocean model simulation of the regional anomaly in sea level trend, 1992-2007. This is generated by subtracting a control run with a 'background' Antarctic freshwater forcing from an experimental run perturbed by an excess Antarctic freshwater runoff of 300 Gt yr⁻¹ (see Suppl. Mat.). The 3000-m isobath is indicated in green.